Published in final edited form as:
Curr Biol. 2014 April 14; 24(8): 832–838. doi:10.1016/j.cub.2014.01.008.

The DEAD box helicase RDE-12 promotes amplification of RNAi in cytoplasmic foci in *C. elegans*

Huan Yang[1,2,§], **Jim Vallandingham**[1], **Philip Shiu**[3], **Hua Li**[1], **Craig P. Hunter**[3], and **Ho Yi Mak**[1,2,¶,*]

[1]Stowers Institute for Medical Research, Kansas City, Missouri 64110, USA

[2]Department of Molecular and Integrative Physiology, University of Kansas Medical Center, Kansas City, Kansas 66160, USA

[3]Department of Molecular and Cellular Biology, Harvard University, Cambridge, Massachusetts 02138, USA

Summary

RNA interference (RNAi) is a potent mechanism for down-regulating gene expression. Conserved RNAi pathway components are found in animals, plants, fungi and other eukaryotes [1–3]. In *C. elegans*, the RNAi response is greatly amplified by the synthesis of abundant secondary siRNAs [4–6]. Exogenous double stranded RNA is processed by Dicer and RDE-1/Argonaute into primary siRNA that guides target mRNA recognition. The RDE-10/RDE-11 complex and the RNA dependent RNA polymerase RRF-1 then engage the target mRNA for secondary siRNA synthesis [7, 8]. However, the molecular link between primary siRNA production and secondary siRNA synthesis remains largely unknown. Furthermore, it is unclear if the sub-cellular sites for target mRNA recognition and degradation coincide with sites where siRNA synthesis and amplification occur. In the *C. elegans* germline, cytoplasmic P granules at the nuclear pores and perinuclear Mutator foci contribute to target mRNA surveillance and siRNA amplification, respectively [9–11]. We report that RDE-12, a conserved FG domain containing DEAD-box helicase, localizes in P-granules and cytoplasmic foci that are enriched in RSD-6 but are excluded from the Mutator foci. Our results suggest that RDE-12 promotes secondary siRNA synthesis by orchestrating the recruitment of RDE-10 and RRF-1 to primary siRNA targeted mRNA in distinct cytoplasmic compartments.

Keywords

RDE-12; siRNA; RNAi; *C. elegans*

*hym@ust.hk.
§Present address: Program in Gene Function and Expression, University of Massachusetts Medical School, Worcester, MA 01605, USA
¶Present address: Division of Life Science, The Hong Kong University of Science and Technology, Hong Kong

Results and Discussion

From a genetic screen for mutants that failed to silence a transgene (*hjIs21*), we identified alleles that define *rde-10*, *rde-11* and *rde-12* [7]. The RDE-10/RDE-11 protein complex is required for secondary siRNA synthesis and triggers RNAi-induced mRNA degradation by association with target mRNA. Here, we report the molecular cloning and characterization of the *rde-12* gene (F58G11.2). The RDE-12 protein is predicted to contain a central DEAD-box RNA helicase domain and an FG domain, found normally in nucleoporins, at the C-terminus (Fig. 1A, Fig. S1A-C). *rde-12* mutant animals were resistant to RNAi against endogenous genes that are normally expressed in the intestine, hypodermis, body wall muscle or germline, when dsRNA triggers were delivered by *E. coli* feeding (Fig. 1B, Fig. S1D, Table S1). Therefore, RDE-12 is broadly required for transgene silencing and exogenous RNAi in *C. elegans*.

Injection of in vitro synthesized *pal-1* double stranded RNA (dsRNA) into the gonad of adult wild type animals normally caused 100% embryonic lethality. While injection of high concentrations of dsRNA (100 and 50 ng/μl) caused a similar phenotype in the majority of *rde-12* progeny (Fig. 1C), *rde-12* mutant animals were significantly less sensitive than wild-type animals when we lowered the dsRNA concentration (10ng/μl). In addition, *rde-12* mutant animals were partially sensitive to RNAi against *act-5* (Fig. S1E). Our results indicate that loss of *rde-12* function causes a dose-dependent defect in RNAi, a phenotype shared by *rde-10* and *rde-11* mutant animals [8].

Many small RNA pathway components are localized to cytoplasmic foci. In mammalian cells, Ago2 is localized to cytoplasmic processing bodies (P bodies) [12], where mRNA deadenylation, decapping and decay occur [13]. In *Drosophila*, the Dcr-2/Dicer interacting protein R2D2 is found in D2 bodies [14]. In *C. elegans*, miRNA loaded Argonaute proteins are localized to P bodies and several other Argonaute proteins and their accessory proteins are localized to the germline specific P granules [15–20]. More recently, the Mutator foci were reported to be a compartment for siRNA amplification in the germline [9].

To determine the localization of RDE-12, we generated single copy transgenes that expressed a functional translational fusion of green fluorescent protein (GFP) and RDE-12. Because these transgenes were able to rescue the Rde phenotype of *rde-12* mutant animals, we inferred that the expression level GFP::RDE-12 was sufficient (Table S1, Fig. S2A). The GFP::RDE-12 protein appeared to localize in discrete cytoplasmic foci in both the soma and germline (Fig. 1D, Fig. S3A). We determined that wild type RDE-12 co-localized with PGL-1 in perinuclear P-granules in the germline (Fig. 1D) [10, 11]. In addition, RSD-6, the Tudor domain containing RNAi effector [21], was enriched in a sub-population of RDE-12 foci in the germline and embryos (Fig. 1E, Fig. S2C). We named these foci R2 bodies because they are enriched in both RDE-12 and RSD-6. In contrast, RDE-12 did not co-localize with DCAP-1 or MUT-14 (Fig. 1F-G, Fig. S2B). Our results indicate that RDE-12 is excluded from cytoplasmic P bodies and perinuclear Mutator foci, two compartments that have been implicated in mRNA turnover and siRNA amplification, respectively [13, 22].

The RDE-12 protein contains two domains: the helicase core domain, which is composed of several functional motifs, including the central DEAD box helicase motif and the SAT motif, and the C-terminal FG domain. We first tested how mutations in each of the core helicase motifs affected RDE-12 localization by expressing GFP::RDE-12 translational fusion proteins that bore the following mutations: DEAD mutated to DQAD and SAT mutated to AAA. Both mutant proteins were expressed at levels comparable to the wild-type rescuing GFP::RDE-12 fusion protein (Fig. S2A). In the germline, the GFP::RDE-12(DQAD) mutant protein showed reduced localization to P-granule foci concomitant with accumulation of large cytoplasmic foci that may represent aggregates (Fig. 2A). In contrast, the localization of the GFP::RDE-12(AAA) mutant was similar to the wild-type GFP::RDE-12 protein (Fig. 2B). These results show that catalytic residues in the helicase domain are not absolutely required for the localization of RDE-12 to P-granules.

In contrast, the proper localization of RDE-12 is dependent on its FG domain. The FG domain is enriched in Phe-Gly (FG) repeats and is found in numerous nuclear pore proteins, which are capable of forming hydrogel that may serve as a selective permeability filter [23, 24]. The GFP::RDE-12 fusion protein deleted for the FG domain (ΔFG) was expressed at levels comparable to the wild-type rescuing GFP::RDE-12 fusion protein (Fig. S2A). However, the majority of GFP::RDE-12(ΔFG) failed to localize to P granules and was found in punctate structures adjacent to P granules instead (Fig. 2C). These punctate structures were also distinct from Mutator foci but were highly enriched with RSD-6 (Fig. 2D–E). Quantitatively, RSD-6 showed significantly stronger co-localization with GFP::RDE-12(ΔFG) than GFP::RDE-12 (Pearson's correlation coefficient: 0.725 versus 0.554, $P<0.005$ t-test). The co-localization of GFP::RDE-12(ΔFG) with RSD-6 was also observed in early embryos (Fig. S2D). Our results indicate that the FG domain is crucial for maintaining the localization of RDE-12 in P-granules.

To determine whether the localization of RDE-12 mutant proteins correlated with their ability to support RNAi, we subjected *rde-12* mutant animals that expressed RDE-12(DQAD), RDE-12(AAA) and RDE-12(ΔFG) to RNAi against the *unc-15* gene. Quantification of *unc-15* mRNA levels indicated that the RDE-12(ΔFG) mutant, which was confined to R2 bodies, failed to rescue the RNAi defective phenotype of *rde-12* mutant animals, while the RDE-12(AAA) or RDE-12(DQAD) mutants conferred partial rescue (Fig. 2F). Similar results were obtained when the same panel of animals was subjected to RNAi against *pos-1*, *mex-3*, *nhr-23*, *elt-2* and *flr-1* genes (Table S1). Mechanistically, the RDE-12(ΔFG) mutant failed to support secondary siRNA synthesis while the RDE-12(AAA) mutant was partially defective (Fig. 2G, see later). Taken together, we favor the model that the FG domain is critical for RDE-12 function by specifying its subcellular localization.

Since RDE-12 is predicted to be an RNA helicase, we hypothesize that RDE-12 may associate with mRNAs that are targeted by RNAi. Indeed, when animals were subjected to RNAi against the *elt-2* or *dpy-28* gene, the respective mRNA was preferentially bound by RDE-12 based on RNA co-immunoprecipitation assays (Fig. 3A). We also found that RSD-6, which co-localized with RDE-12 in R2 bodies, specifically associated with mRNAs

that were targeted by RNAi (Fig. 3B). The lower fold-enrichment of RSD-6 with target mRNAs may reflect a more transient nature of their association with RSD-6 than RDE-12.

Next, we determined whether RDE-12 required other RNAi pathway components to associate with target mRNAs. Specifically, we performed RDE-12 RNA IP in *rde-1*, *rde-10* and *rrf-1* mutant animals that were subjected to RNAi against the endogenous *sel-1* gene. The maturation of primary siRNA is blocked in *rde-1* mutant animals while secondary siRNA synthesis in somatic tissues is impaired in *rde-10* and *rrf-1* mutant animals [6, 25]. We found that RDE-12 could engage target mRNAs in *rrf-1* and *rde-10* mutant animals but failed to do so in *rde-1* mutant animals (Fig. 3C). Similar observations were made when a second endogenous gene, *flr-1*, was targeted by RNAi (HUY, unpublished data). Our results indicate that the association of target mRNA by RDE-12 requires primary siRNAs. RDE-12 in turns acts upstream of RDE-10: the association of RDE-10 with target mRNAs was reduced by 80% in *rde-12* mutant animals (Fig. 3D).

To probe the molecular basis that underlies the exogenous RNAi defect in *rde-12* mutant animals, we subjected wild type and *rde-12* mutant animals to RNAi against a somatic gene, *sel-1*, and profiled small RNAs from two independent populations of synchronized young adult animals of each genotype by deep sequencing (Fig. 4A). Each biological sample yielded, on average, ~29 million mapped reads (Fig. S4A-H). We found that *rde-12* mutant animals contained ~50% more primary siRNAs and 60-fold less secondary siRNAs than wild-type animals (Fig. 4B-C, Table S2). Similar results were observed in *rde-10*, *rde-11* mutant animals [7, 8]. Therefore, RDE-12 is necessary for secondary but not primary siRNA biogenesis.

Unlike exogenous siRNAs, endogenous siRNAs (endo-siRNAs) are derived from native genomic loci [26, 27]. Based on the length and 5′ nucleotide of the endo-siRNAs and their interacting Argonaute proteins, endo-siRNA pathways can generally be classified into ERGO-1 26G, ALG-3/4 26G, WAGO-1 22G and CSR-1 22G pathways [16, 17, 19, 28, 29]. These pathways target different populations of genes with little overlap. We measured the abundance of small RNAs in each of the four endo-siRNA pathways in wild type and *rde-12* mutant animals by deep sequencing (Dataset S1), and compiled the results in a MA plot (Fig. 4D). The abundance of CSR-1 and ALG-3/4 classes of endo-siRNA remained unchanged. However, we detected more than 2-fold reduction of endo-siRNAs in 38 out of 56 ERGO-1 targets and 29 out of 1,110 WAGO-1 targets in *rde-12* mutant animals (Dataset S1). Among the 29 targets of WAGO-1 endo-siRNAs, 8 of them also belong to the ERGO-1 class (Dataset S1), and several are classified as targets of soma-enriched endo-siRNAs (for example: Y47H10A.5) [19, 30]. Taking the entire class of endo-siRNAs into consideration, the expression level of the ERGO-1 class was reduced, while the CSR-1, ALG-3/4 and WAGO-1 classes were not significantly affected in *rde-12* mutant animals (Fig. 4E).

ERGO-1 associated 26G RNAs can trigger the generation of a secondary pool of 22G RNAs, similar to the amplification of exogenous siRNAs [29, 31]. We focused our analysis on 26G RNAs that were derived from 23 previously characterized endogenous targets (Dataset S2 and Fig. S4I) [31]. We found that the expression level of the most abundant members of this group remained unchanged in *rde-12* mutant animals. However, the level of

their corresponding 22G RNAs was reduced by more than 4-fold (Fig. 4F). Accordingly, the expression level of five out of six target genes of these 22G endo-siRNAs was increased in *rde-12* mutant animals (Fig. 4G). This phenotype could be rescued by a wild-type *rde-12* transgene. Taken together, our results indicate that RDE-12 is required for secondary amplification of the ERGO-1 class of endo-siRNAs, which mirrors its role in promoting secondary siRNA synthesis in the exogenous RNAi pathway.

In addition to endo-siRNAs, miRNA and piRNA are abundant small RNAs that are derived from non-coding genomic loci [2, 26, 27, 32, 33]. We compared the representation of miRNA and piRNA in wild type versus *rde-12* mutant animals in our deep sequencing data sets. We found that the expression of <0.1% miRNA and piRNA was reduced in *rde-12* mutant animals. Therefore, RDE-12 is not required for the biogenesis of most if not all miRNA and piRNA. Accordingly, *rde-12* mutant animals do not have heterochronic or developmental defects that are commonly associated with loss of miRNA function.

In this paper, we identify the DEAD-box helicase RDE-12 as a critical factor for secondary siRNA synthesis and efficient RNAi in *C. elegans*. Our genetic and genomic analyses indicate that RDE-12 engages target mRNA downstream of RDE-1/Argonaute, and promotes subsequent recruitment of the RDE-10/RDE-11 complex [7], prior to secondary siRNA synthesis by RRF-1/RdRP. RDE-12 appears to define discrete cytoplasmic foci that are distinct from P bodies and Mutator foci. A sub-population of RDE-12 foci (R2 bodies) is also enriched with the Tudor domain protein RSD-6, suggesting fine spatial division of cytoplasmic compartments for target mRNA engagement and siRNA synthesis. Although repeated attempts to visualize RDE-10 and RDE-11 were unsuccessful, it is plausible that they are present in R2 bodies since RSD-2 can physically associate with RSD-6 and RDE-10 [7, 8, 21]. We propose a model that the surveillance of mRNA targets, siRNA synthesis, and mRNA degradation occur in multiple populations of peri-nuclear foci in the germline and their cytoplasmic counterparts in the soma (Fig. S1F). It is plausible that RDE-12 shuttles primary siRNA bound target mRNAs from P granules to RSD-6 positive foci (R2 bodies) where secondary siRNA synthesis is initiated. The hand-over of target mRNA by RDE-12 to RDE-10 in R2 bodies may then be followed by FG domain dependent recycling of RDE-12 to the P-granules. Our model predicts that RDE-12 associates with RDE-1, RDE-10 and RSD-6 transiently, perhaps through their co-occupancy of target mRNAs. Taken together, our work reveals unexpected complexity in the molecular and sub-cellular mechanisms for the amplification of RNAi response in *C. elegans*.

Supplementary Material

Refer to Web version on PubMed Central for supplementary material.

Acknowledgments

We are grateful to Peter Baumann for providing space and equipment to H.Y. for completing this study. We thank Marco Blanchette for assistance in the preparation of Fig. 4D and 4E; Sean McKinney for image analysis; Carolyn Phillips and Gary Ruvkun for strains; Peter Baumann and Marco Blanchette for helpful discussions. This work was performed to fulfill, in part, requirements for H.Y.'s PhD dissertation research as a student registered with the University of Kansas Medical Center. This work was funded by the Stowers Institute for Medical Research (H.Y.M.) and by the National Institutes of Health (C.P.H.). H.Y. was responsible for the design and execution of

experiments in all figures, supplemental figures and supplemental tables except for Fig. 1C and Fig. S1D-E, which were contributed by P.S. and C.P.H.. J.V. and H.L. performed deep-sequencing data analysis for Fig. 4, Fig. S4, and Table S2 with input from H.Y.. H.Y.M. conducted the genetic screen and contributed to experimental design. H.Y. and H.Y.M. wrote the manuscript with input from C.P.H..

References

1. Ghildiyal M, Zamore PD. Small silencing RNAs: an expanding universe. Nat Rev Genet. 2009; 10:94–108. [PubMed: 19148191]
2. Ketting RF. The many faces of RNAi. Developmental cell. 2011; 20:148–161. [PubMed: 21316584]
3. Malone CD, Hannon GJ. Small RNAs as guardians of the genome. Cell. 2009; 136:656–668. [PubMed: 19239887]
4. Pak J, Fire A. Distinct populations of primary and secondary effectors during RNAi in C. elegans. Science. 2007; 315:241–244. [PubMed: 17124291]
5. Sijen T, Fleenor J, Simmer F, Thijssen KL, Parrish S, Timmons L, Plasterk RH, Fire A. On the role of RNA amplification in dsRNA-triggered gene silencing. Cell. 2001; 107:465–476. [PubMed: 11719187]
6. Yigit E, Batista PJ, Bei Y, Pang KM, Chen CC, Tolia NH, Joshua-Tor L, Mitani S, Simard MJ, Mello CC. Analysis of the C. elegans Argonaute family reveals that distinct Argonautes act sequentially during RNAi. Cell. 2006; 127:747–757. [PubMed: 17110334]
7. Yang H, Zhang Y, Vallandingham J, Li H, Florens L, Mak HY. The RDE-10/RDE-11 complex triggers RNAi-induced mRNA degradation by association with target mRNA in C. elegans. Genes & development. 2012; 26:846–856. [PubMed: 22508728]
8. Zhang C, Montgomery TA, Fischer SE, Garcia SM, Riedel CG, Fahlgren N, Sullivan CM, Carrington JC, Ruvkun G. The Caenorhabditis elegans RDE-10/RDE-11 complex regulates RNAi by promoting secondary siRNA amplification. Current biology : CB. 2012; 22:881–890. [PubMed: 22542102]
9. Phillips CM, Montgomery TA, Breen PC, Ruvkun G. MUT-16 promotes formation of perinuclear mutator foci required for RNA silencing in the C. elegans germline. Genes & development. 2012; 26:1433–1444. [PubMed: 22713602]
10. Sheth U, Pitt J, Dennis S, Priess JR. Perinuclear P granules are the principal sites of mRNA export in adult C. elegans germ cells. Development. 2010; 137:1305–1314. [PubMed: 20223759]
11. Updike D, Strome S. P granule assembly and function in Caenorhabditis elegans germ cells. J Androl. 2010; 31:53–60. [PubMed: 19875490]
12. Sen GL, Blau HM. Argonaute 2/RISC resides in sites of mammalian mRNA decay known as cytoplasmic bodies. Nat Cell Biol. 2005; 7:633–636. [PubMed: 15908945]
13. Parker R, Sheth U. P bodies and the control of mRNA translation and degradation. Molecular cell. 2007; 25:635–646. [PubMed: 17349952]
14. Nishida KM, Miyoshi K, Ogino A, Miyoshi T, Siomi H, Siomi MC. Roles of R2D2, a cytoplasmic D2 body component, in the endogenous siRNA pathway in Drosophila. Molecular cell. 2013; 49:680–691. [PubMed: 23375501]
15. Batista PJ, Ruby JG, Claycomb JM, Chiang R, Fahlgren N, Kasschau KD, Chaves DA, Gu W, Vasale JJ, Duan S, et al. PRG-1 and 21U-RNAs interact to form the piRNA complex required for fertility in C. elegans. Molecular cell. 2008; 31:67–78. [PubMed: 18571452]
16. Claycomb JM, Batista PJ, Pang KM, Gu W, Vasale JJ, van Wolfswinkel JC, Chaves DA, Shirayama M, Mitani S, Ketting RF, et al. The Argonaute CSR-1 and its 22G-RNA cofactors are required for holocentric chromosome segregation. Cell. 2009; 139:123–134. [PubMed: 19804758]
17. Conine CC, Batista PJ, Gu W, Claycomb JM, Chaves DA, Shirayama M, Mello CC. Argonautes ALG-3 and ALG-4 are required for spermatogenesis-specific 26G-RNAs and thermotolerant sperm in Caenorhabditis elegans. Proceedings of the National Academy of Sciences of the United States of America. 2010; 107:3588–3593. [PubMed: 20133686]
18. Ding L, Spencer A, Morita K, Han M. The developmental timing regulator AIN-1 interacts with miRISCs and may target the argonaute protein ALG-1 to cytoplasmic P bodies in C. elegans. Molecular cell. 2005; 19:437–447. [PubMed: 16109369]

19. Gu W, Shirayama M, Conte D Jr, Vasale J, Batista PJ, Claycomb JM, Moresco JJ, Youngman EM, Keys J, Stoltz MJ, et al. Distinct argonaute-mediated 22G-RNA pathways direct genome surveillance in the C. elegans germline. Molecular cell. 2009; 36:231–244. [PubMed: 19800275]
20. van Wolfswinkel JC, Claycomb JM, Batista PJ, Mello CC, Berezikov E, Ketting RF. CDE-1 affects chromosome segregation through uridylation of CSR-1-bound siRNAs. Cell. 2009; 139:135–148. [PubMed: 19804759]
21. Tijsterman M, May RC, Simmer F, Okihara KL, Plasterk RH. Genes required for systemic RNA interference in Caenorhabditis elegans. Current biology : CB. 2004; 14:111–116. [PubMed: 14738731]
22. Eulalio A, Behm-Ansmant I, Schweizer D, Izaurralde E. P-body formation is a consequence, not the cause, of RNA-mediated gene silencing. Mol Cell Biol. 2007; 27:3970–3981. [PubMed: 17403906]
23. Frey S, Richter RP, Gorlich D. FG-rich repeats of nuclear pore proteins form a three-dimensional meshwork with hydrogel-like properties. Science. 2006; 314:815–817. [PubMed: 17082456]
24. Labokha AA, Gradmann S, Frey S, Hulsmann BB, Urlaub H, Baldus M, Gorlich D. Systematic analysis of barrier-forming FG hydrogels from Xenopus nuclear pore complexes. The EMBO journal. 2013; 32:204–218. [PubMed: 23202855]
25. Pak J, Maniar JM, Mello CC, Fire A. Protection from feed-forward amplification in an amplified RNAi mechanism. Cell. 2012; 151:885–899. [PubMed: 23141544]
26. Ambros V, Lee RC, Lavanway A, Williams PT, Jewell D. MicroRNAs and other tiny endogenous RNAs in C. elegans. Current biology : CB. 2003; 13:807–818. [PubMed: 12747828]
27. Ruby JG, Jan C, Player C, Axtell MJ, Lee W, Nusbaum C, Ge H, Bartel DP. Large-scale sequencing reveals 21U-RNAs and additional microRNAs and endogenous siRNAs in C. elegans. Cell. 2006; 127:1193–1207. [PubMed: 17174894]
28. Han T, Manoharan AP, Harkins TT, Bouffard P, Fitzpatrick C, Chu DS, Thierry-Mieg D, Thierry-Mieg J, Kim JK. 26G endo-siRNAs regulate spermatogenic and zygotic gene expression in Caenorhabditis elegans. Proceedings of the National Academy of Sciences of the United States of America. 2009; 106:18674–18679. [PubMed: 19846761]
29. Vasale JJ, Gu W, Thivierge C, Batista PJ, Claycomb JM, Youngman EM, Duchaine TF, Mello CC, Conte D Jr. Sequential rounds of RNA-dependent RNA transcription drive endogenous small-RNA biogenesis in the ERGO-1/Argonaute pathway. Proceedings of the National Academy of Sciences of the United States of America. 2010; 107:3582–3587. [PubMed: 20133583]
30. Fischer SE, Montgomery TA, Zhang C, Fahlgren N, Breen PC, Hwang A, Sullivan CM, Carrington JC, Ruvkun G. The ERI-6/7 helicase acts at the first stage of an siRNA amplification pathway that targets recent gene duplications. PLoS Genet. 2011; 7:e1002369. [PubMed: 22102828]
31. Gent JI, Lamm AT, Pavelec DM, Maniar JM, Parameswaran P, Tao L, Kennedy S, Fire AZ. Distinct phases of siRNA synthesis in an endogenous RNAi pathway in C. elegans soma. Molecular cell. 2010; 37:679–689. [PubMed: 20116306]
32. Carthew RW, Sontheimer EJ. Origins and Mechanisms of miRNAs and siRNAs. Cell. 2009; 136:642–655. [PubMed: 19239886]
33. Hutvagner G, Simard MJ. Argonaute proteins: key players in RNA silencing. Nat Rev Mol Cell Biol. 2008; 9:22–32. [PubMed: 18073770]

Highlights

- The DEAD-box RNA helicase RDE-12 promotes secondary siRNA synthesis in *C. elegans*
- RDE-12 localizes to P granules and RSD-6 rich R2 bodies for RNAi amplification
- RDE-12 associates with RNAi targeted mRNA downstream of primary siRNA production
- RDE-12 is required for target mRNA engagement by RDE-10 and RRF-1/RdRP

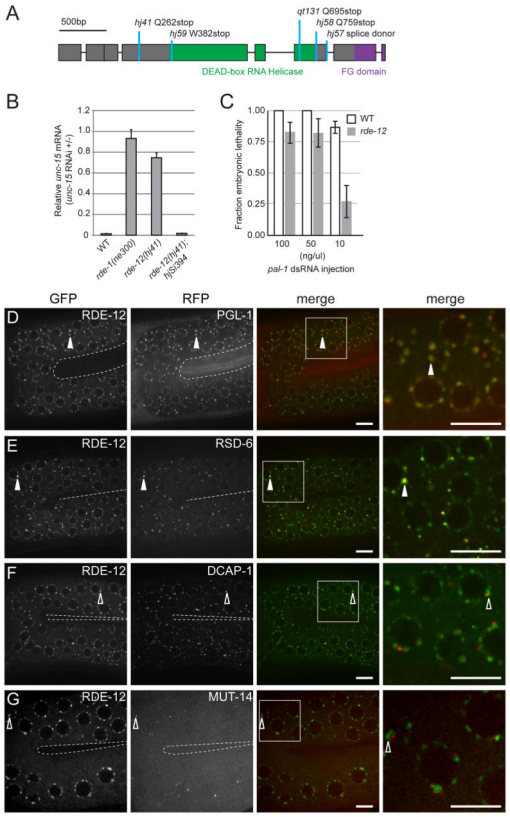

Figure 1. *rde-12* is required for RNAi and is localized to P granules

(A) Gene structure of *rde-12*. Exons are depicted in boxes. Mutant alleles and corresponding changes in the protein sequence are indicated. (B) Relative abundance of endogenous *unc-15* mRNA in synchronized wild-type (WT), *rde-1(ne300)*, *rde-12(hj41)* and *rde-12(hj41); hjSi394[rde-12(+)]* animals subjected to *unc-15* RNAi compared to no RNAi control (L4440 vector). Mean + standard deviation from three independent samples assayed in triplicates are shown. (C) *rde-12(qt131)* animals were sensitive to RNAi against *pal-1* when high doses of dsRNA were directly injected into the gonad. Number of injected animals n=8–17. Mean ± standard deviation. At 100 and 50ng/μl, wild type and *rde-12* mutant animals were not significantly different. At 10ng/μl, $p<0.01$. (D–G) The germline (in the loop region connecting the proximal and distal gonad arms) of live animals were imaged by confocal microscopy. The inner border of gonad arms is depicted by dotted lines. Full-length RDE-12 was fused to GFP (GFP::RDE-12). (D) mRuby::PGL-1; (E) tagRFP::RSD-6; (F) mRuby::DCAP-1; (G) MUT-14::mCherry. Solid arrowheads indicate co-localization of GFP with RFP signals. Open arrowheads indicate the positions of GFP signals that do not overlap with RFP signals. Boxed areas were magnified 3x and shown in the far right panels. Scale bars, 6.5μm.

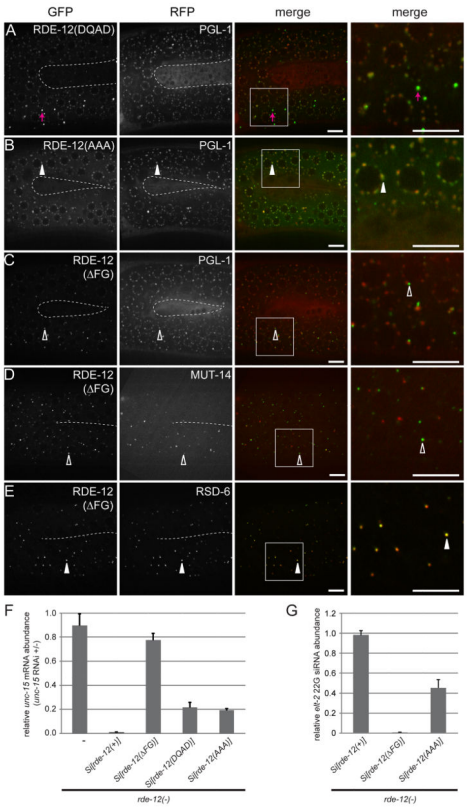

Figure 2. The FG domain is required for proper RDE-12 localization

(A–E) The germline (in the loop region connecting the proximal and distal gonad arms) of live animals were imaged by confocal microscopy. The inner border of gonad arms is depicted by dotted lines. Boxed areas were magnified 3x and shown in the far right panels. (A–C) mRuby::PGL-1 and translational fusion of GFP with mutant forms of RDE-12. (A) DEAD motif mutated to DQAD, abnormal GFP aggregates are indicated by magenta arrows; (B) SAT motif mutated to AAA; (C) FG domain (amino acid residues 875-959) deleted. (D) GFP::RDE-12(ΔFG) and MUT-14::mCherry (Mutator foci marker). (E) GFP::RDE-12(ΔFG) and RSD-6. Solid arrowheads indicate co-localization of GFP with RFP signals. Open arrowheads indicate the positions of GFP signals that do not overlap with RFP signals. Boxed areas were magnified 3x and shown in the far right panels. Scale bars, 6.5μm. (F) Relative abundance of endogenous *unc-15* mRNA in synchronized *rde-12(hj41)* mutant animals carrying the indicated transgeneswhen they were subjected to *unc-15* RNAi compared to no RNAi control (L4440 vector). Mean + standard deviation from three independent samples assayed in triplicates is shown. (G) Relative abundance of *elt-2* 22G secondary siRNA in synchronized *rde-12(hj41)* mutant animals carrying the indicated transgenes when they were subjected to *elt-2* RNAi. Mean + standard deviation from three independent samples assayed in triplicates is shown.

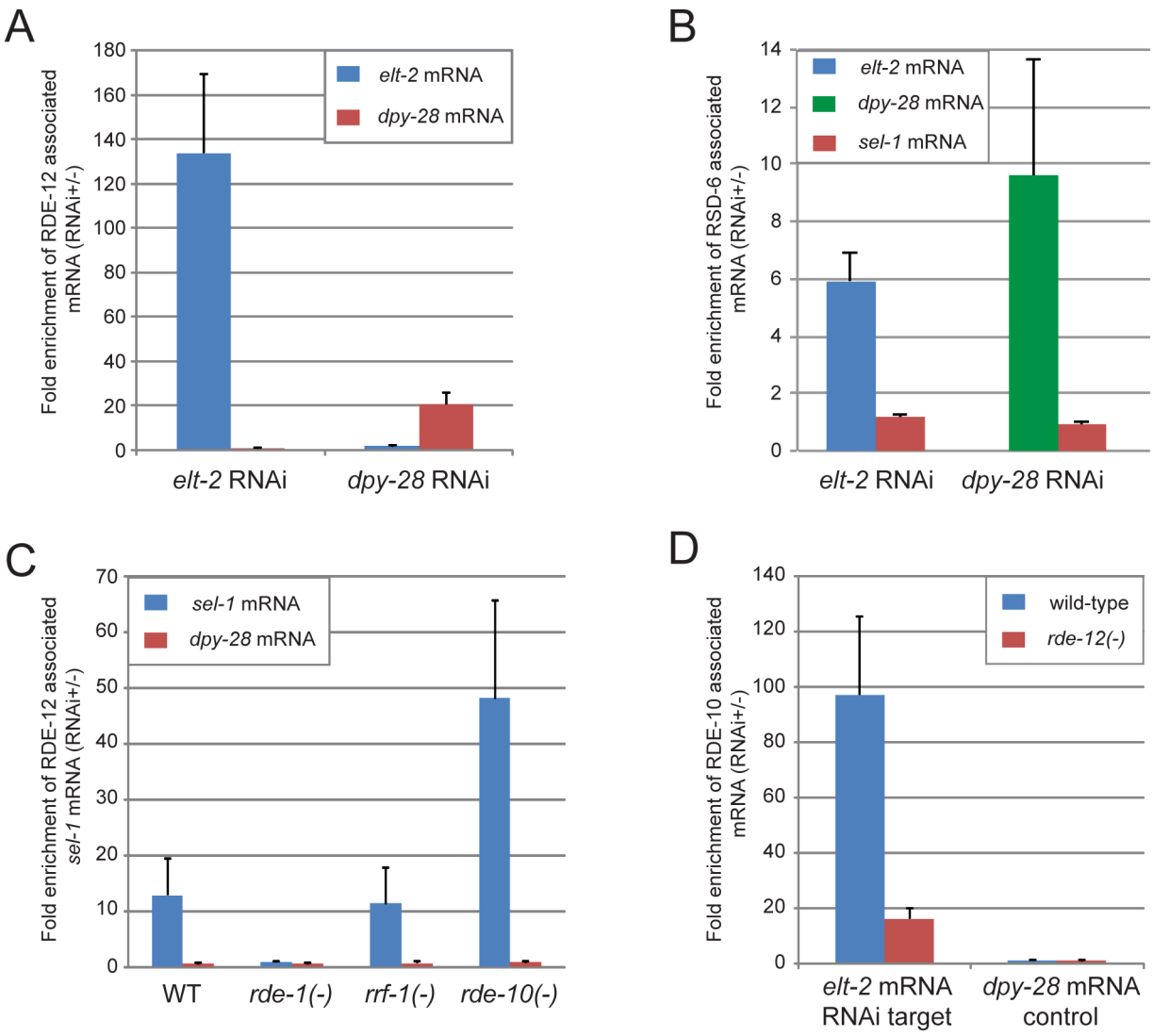

Figure 3. RDE-12 and RSD-6 associate with mRNA targeted by RNAi

(A) Target mRNA preferentially associated with RDE-12 in response to *elt-2* RNAi or *dpy-28* RNAi. Abundance of mRNA was measured by real-time PCR. (B) Target mRNA preferentially associated with RSD-6 in response to *elt-2* RNAi or *dpy-28* RNAi. Abundance of mRNA was measured by real-time PCR. The *sel-1* mRNA, which was not targeted by RNAi, served as a negative control. (C) Target *sel-1* mRNA preferentially associated with RDE-12 in wild-type (WT), *rde-10(hj20)*, *rrf-1(pk1417)* but not *rde-1(ne300)* animals. (D) The association of RDE-10 with target mRNAs was reduced in *rde-12* mutant animals. All results are shown as mean + standard deviation from at least three independent biological samples assayed in triplicates.

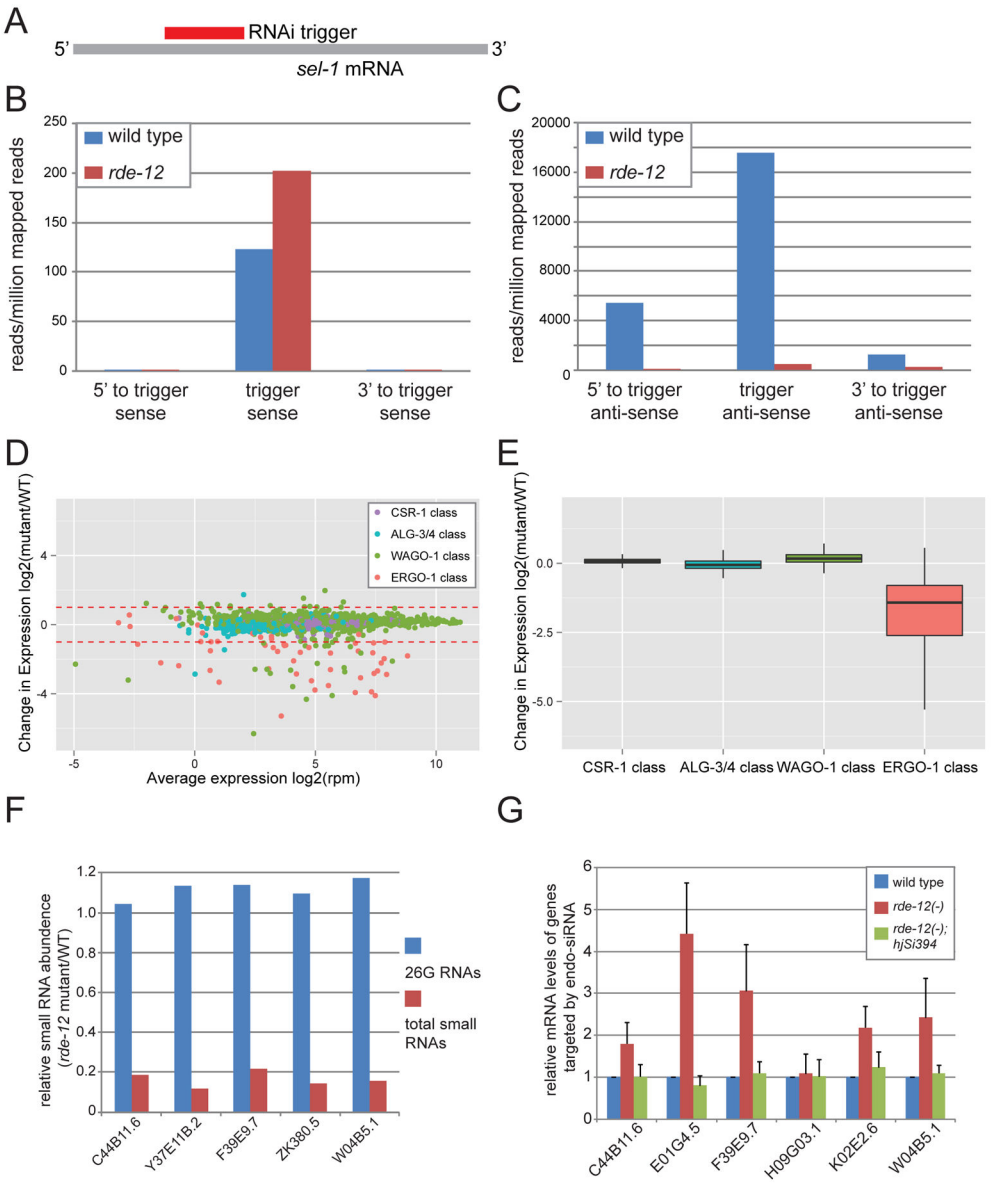

Figure 4. RDE-12 is required for secondary siRNA synthesis

(A) Schematic representation of the *sel-1* RNAi trigger and *sel-1* mRNA. (B–C) The mean abundance of small RNAs from two independent populations of wild-type and *rde-12(hj41)* animals undergoing *sel-1* RNAi is shown. (B) Sense *sel-1* siRNAs. (C) Antisense *sel-1* siRNAs. (D) MA plot showing abundance change of endo-siRNA in individual targets of ALG-3/4, CSR-1, ERGO-1 and WAGO-1. (E) Relative abundance of endo-siRNAs in wild-type (WT) versus *rde-12* mutant animals. (F) The relative abundance of 26G RNAs and total endo-siRNAs in target genes of the somatic ERGO-1 pathway (WT=1.0). All listed target genes have >1 RPM 26G RNAs. (G) Relative abundance of endogenous mRNAs targeted by the ERGO-1 class 26G siRNAs in wild type, *rde-12(hj41)* and *rde-12(hj41);hjSi394[rde-12(+)]* animals as determined by real-time PCR (WT = 1.0).